

Quantum-electrodynamic radiative corrections to the decay $\pi^0 \rightarrow \gamma e^+ e^-$

L. Roberts and J. Smith

Institute for Theoretical Physics, State University of New York at Stony Brook, Stony Brook, New York 11794-3840

(Received 27 November 1985)

The quantum-electrodynamic radiative corrections to both the decay rate for $\pi^0 \rightarrow \gamma e^+ e^-$ and the differential spectrum in the invariant mass of the Dalitz pair for experiments with limited geometrical acceptance are calculated.

The decay $\pi^0 \rightarrow \gamma e^+ e^-$ presents an opportunity to study strong-interaction effects at the $\pi^0 \gamma \gamma$ vertex when one γ is virtual. These effects are parametrized by introducing a form factor at the vertex and expanding it in a Taylor series in powers of x , the invariant mass of the Dalitz pair divided by $m_{\pi^0}^2$, i.e., $f(x) = 1 + ax + \dots$. Experimental determinations of a have given $a = 0.10 \pm 0.03$ (Ref. 1), $a = 0.01 \pm 0.11$ (Ref. 2), $a = -0.15 \pm 0.10$ (Ref. 3), and $a = -0.24 \pm 0.16$ (Ref. 4). The recent measurement of Ref. 1 came from a study of 30 000 $\pi^0 \rightarrow \gamma e^+ e^-$ events produced via $K_{\pi_2}^+$ decays in flight. The group determined that a changed from $a = 0.05 \pm 0.03$ in the absence of radiative corrections to $a = 0.10 \pm 0.03$ when radiative corrections were included. This change by a factor of 2 shows these corrections to be extremely important. Since the previous measurements did not include radiative corrections, the numbers in Refs. 2–4 should no longer be given much weight. Nevertheless, the theoretical expectations for a based on vector-meson dominance and dispersion theory yield $a = 0.031$ (Ref. 5) and $a = 0.046$ (Ref. 6) which still disagree with the experimental result of Ref. 1. To hopefully clarify the situation, a new experiment has been performed at TRIUMF⁷ and the data are presently being analyzed. The experiment studies $\pi^0 \rightarrow \gamma e^+ e^-$ decays from a stopped π^- beam in a liquid-hydrogen target, with the energies of the electron-positron pair determined by two large NaI detectors and their opening angle by wire chambers. With the limited angular acceptance and the possibility of the direct and/or radiative photons entering the NaI detectors and distorting the lepton energy measurement, it is not possible to modify the published radiative-correction calculations^{8,9} to cover this new situation. Therefore, we have recalculated them and have written two computer programs to allow the calculation of the radiative corrections for $\pi^0 \rightarrow \gamma e^+ e^-$ for any experimental situation. In this paper we present an outline of our work and give some numerical results.

The decay amplitude for $\pi^0 \rightarrow \gamma e^+ e^-$ is represented in lowest order by the Feynman diagram in Fig. 1. Radiative corrections to $\pi^0 \rightarrow \gamma e^+ e^-$ come from two sources: (1) virtual corrections and (2) bremsstrahlung corrections. The virtual corrections come from the interference of the amplitude for the one-loop Feynman diagrams in Fig. 2 with the lowest-order amplitude in Fig. 1. The bremsstrahlung corrections involve the square of the amplitude for the other two Feynman diagrams shown in Fig. 2 and their counterparts obtained by exchanging the radiative and decay photons. Both sets of diagrams were previously considered in Ref. 8, where the radiative corrections to the Dalitz plot for $\pi^0 \rightarrow \gamma e^+ e^-$ were presented and in Ref. 9, where the

corrections to the total decay rate were examined. We used the algebraic program SCHOONSCHIP¹⁰ to reevaluate the bremsstrahlung corrections as a check of the results in Ref. 8 and to simplify code generation for the computer programs.

Before discussing our calculations, we should note that there has recently been a discussion^{11,12} of the necessity of including the interference between the two-virtual-photon loop graphs in Fig. 3 with the graph in Fig. 1 in radiative corrections to $\pi^0 \rightarrow \gamma e^+ e^-$ decay. Although the analysis in Ref. 12 shows that these additional terms have factors of $m_e^2/m_{\pi^0}^2$ and are therefore negligible, this conclusion has been challenged by Tupper and independently by Beder.¹³ If this additional interference term does not have the $m_e^2/m_{\pi^0}^2$ suppression factor, it may be necessary to take it into account. Since the calculation of the graphs in Fig. 3 requires a complete knowledge of the $\pi^0 \rightarrow e^+ e^-$ amplitude together with bremsstrahlung and direct-emission terms, it is clear that results for the interference terms are model dependent. They have not been included in our analysis.

A general radiative-correction program which is suitable for experiments with limited geometrical acceptance requires all integrations to be done numerically. In the absence of infrared divergences, this would be a trivial task. The virtual corrections require simulation of the interference terms over a three-body phase space, whereas the real corrections require simulation of the square of an amplitude over a four-body phase space. Infrared divergences complicate the situation since they must be canceled before the events are simulated in their separate phase spaces; attempting to cancel the divergences after simulation would be impractical due to numerical inaccuracies.

In a previous calculation reported in Ref. 8, some of the phase-space integrations were done analytically. Since all

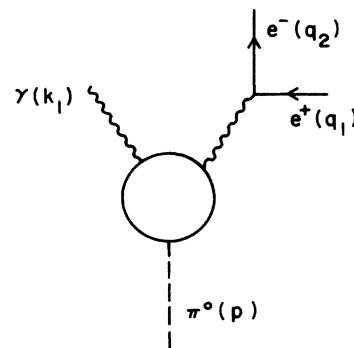


FIG. 1. Lowest-order Feynman diagram for $\pi^0 \rightarrow \gamma e^+ e^-$.

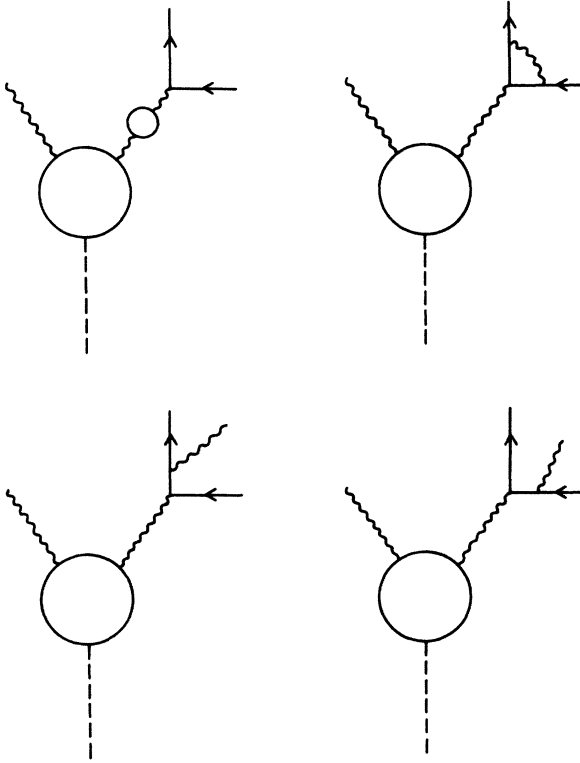


FIG. 2. Higher-order virtual and bremsstrahlung diagrams contributing to π^0 decay.

experiments concentrate on the measurement of the spectrum in the Dalitz-pair invariant mass, it was useful to keep this as the last integration variable. Hence, for the bremsstrahlung reaction, convenient variables to use were $x = (q_1 + q_2)^2/m_{\pi^0}^2$, $y = 2p \cdot (q_1 - q_2)/[m_{\pi^0}^2(1-x)]$ (the Dalitz-plot variables), and $x_\gamma = (k_1 + k_2)^2/m_{\pi^0}^2$ (the photon-photon invariant mass). The other angular integrations were done analytically in a convenient rest frame, so the geometrical information on the angles of emission of the photons was lost. The infrared divergence was then isolated in specific terms for small values of x_γ . These terms could be extracted, integrated, and the logarithmic divergence canceled with the corresponding divergence in the virtual contribution. The remaining x_γ dependence was integrated numerically over its full range to produce the radiative corrections at points across the x, y Dalitz plot. However, the results of this theoretical study are not really appropriate for an experiment with limited geometrical acceptance, so we have adopted a different strategy.

The simulation of the radiative corrections is now done by integrating over three- and four-body phase-space angles and energies. We then form invariants such as x , y , and x_γ

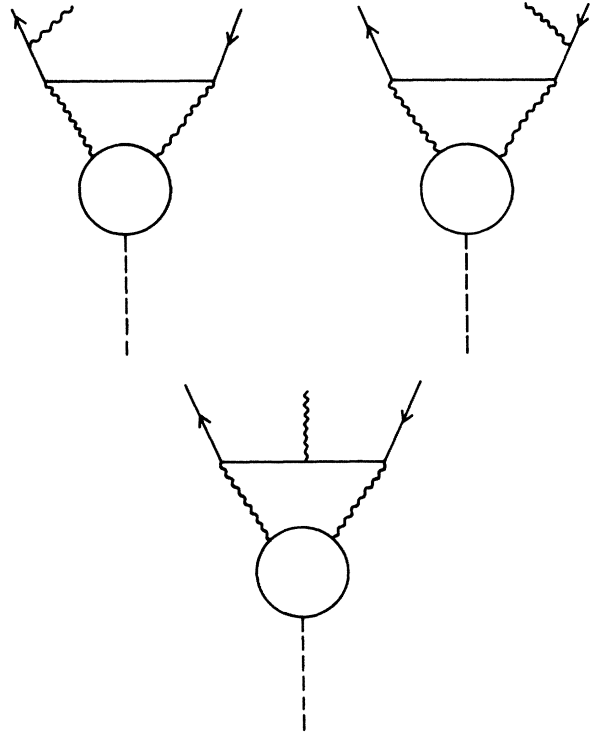


FIG. 3. Higher-order diagrams with two virtual photons.

mentioned above. To handle the infrared-divergent terms in the bremsstrahlung corrections, we rely on the previous methods and integrals given in Ref. 8. Namely, we perform a cut, on the divergent terms only, for x_γ less than some parameter Δ . We then repeated the analytic integration of these terms for $x_\gamma < \Delta$ and added them to the virtual corrections. This means that the infrared-divergent terms are exactly canceled, but the virtual corrections contain a finite piece of the bremsstrahlung corrections depending on Δ , the upper limit of the x_γ integration. Since this is done pointwise across the Dalitz plot, there is the possibility that $(x_\gamma)_{\max} < \Delta$ in certain regions; if this is true, we cut at $(x_\gamma)_{\max}$. Since Δ is the lower limit on the x_γ integration of some (previously divergent) terms in the bremsstrahlung corrections, both contributions are therefore Δ dependent. However, Δ is an *ad hoc* mathematical parameter with no physical significance, so the sum of the two contributions should be Δ independent, even though we can change the relative contributions drastically by choosing unreasonable values of Δ . We can check this assertion by calculating the total radiative correction to the decay rate and comparing the answer with the correction to the (numerically integrated) total rate reported in Ref. 8, and the corresponding analytic formula given in Ref. 9, i.e.,

$$\frac{\Gamma^{\text{rad}}(\pi^0 \rightarrow \gamma e^+ e^-)}{\Gamma(\pi^0 \rightarrow \gamma \gamma)} = \left(\frac{\alpha}{\pi}\right)^2 \left[\frac{8}{9} \ln^2\left(\frac{m_{\pi^0}}{m_e}\right) - \left(\frac{19}{9} - \frac{4}{9}a\right) \ln\left(\frac{m_{\pi^0}}{m_e}\right) + 2\zeta(3) - \frac{2}{27}\pi^2 + \frac{137}{81} - \frac{63}{108}a + O\left(\frac{m_e}{m_{\pi^0}}\right) \right]. \quad (1)$$

Figure 4 presents the total radiative corrections calculated for several values of the parameter Δ to show that our results are Δ independent. Choosing $\Delta = 20m_e^2/m_{\pi^0}^2$, we found that

$$\frac{\Gamma^{\text{rad}}(\pi^0 \rightarrow \gamma e^+ e^-)}{\Gamma(\pi^0 \rightarrow \gamma \gamma)} = 1.024 \times 10^{-4} (\pm 1.2\%) \quad (2)$$

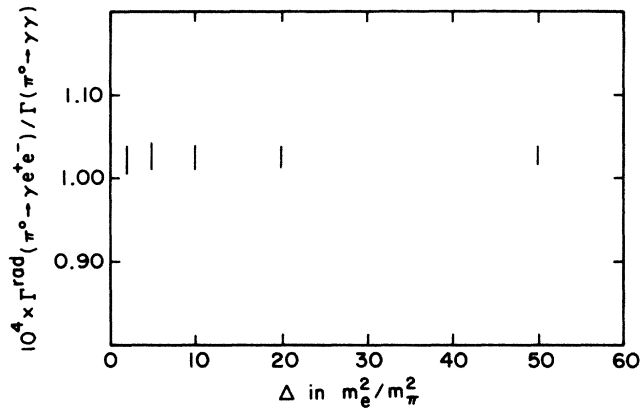


FIG. 4. Δ dependence of the total radiative corrections, $\Gamma^{\text{rad}}(\pi^0 \rightarrow \gamma e^+ e^-) / \Gamma(\pi^0 \rightarrow \gamma\gamma)$.

while the analytic formula (1) with $a=0$ and updated values for $m_{\pi^0} = 134.9626$ MeV, $m_e = 0.511$ MeV, and $\alpha^{-1} = 137.036$ yields

$$\frac{\Gamma^{\text{rad}}(\pi^0 \rightarrow \gamma e^+ e^-)}{\Gamma(\pi^0 \rightarrow \gamma\gamma)} = 1.038 \times 10^{-4} \quad (3)$$

Hence, our computer simulation for the total decay rate yields answers correct to about 1%, which is sufficient for our purposes, since we can achieve better accuracy on a limited phase-space region.

Now it is easy to handle the corrections for any experimental situation. For example, take the recent measurement at TRIUMF. The detector consists of two NaI detectors subtending fixed angles with respect to the π^0 decay po-

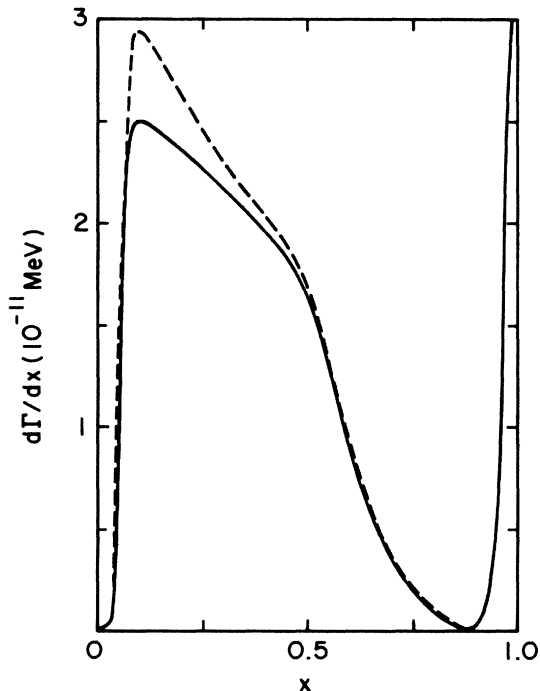


FIG. 5. True distribution in x compared to that of x_{vis} for the lowest-order process. x is shown by the dashed curve; x_{vis} is shown by the solid curve.

sition. Energy thresholds for the electron and positron are known. We force one lepton to enter each detector by simple geometrical cuts. Then, if the photons emerge at angles where they enter the detectors, they are also counted in the energy deposition. Since the angular positions of the electron and positron are known, we simply calculate a spectrum in $x_{\text{vis}} = (2m_e^2 + 2E_1E_2 - 2p_1p_2 \cos\theta) / m_{\pi^0}^2$, where the E_i refer to the energy deposited in each detector, the $p_i = (E_i^2 - m_e^2)^{1/2}$ are the apparent lepton momenta, and θ is the opening angle of the lepton pair. This distribution differs from that of the true x since the radiated photons change the values of the energies deposited. However, since the Monte Carlo program has exact energies and angles, we also know the true x distribution, which should resemble Fig. 4 in Ref. 8.

To illustrate these remarks, we consider the situation where the NaI detectors subtend an angle of 156° . In Fig. 5 we compare the true x vs x_{vis} distributions in the absence of radiative corrections to show the influence of the detector geometry. The true x distribution is modified from the expected $(1-x)^2/x$ behavior (for a full acceptance) by a reduction of events due to the acceptance cut for low values of x . Its shape is as expected. The x_{vis} distribution shows an additional diminution of events near low x_{vis} together with an accumulation of events near $x_{\text{vis}} = 1$, i.e., events are shifted toward $x_{\text{vis}} = 1$. Since the opening angle between the

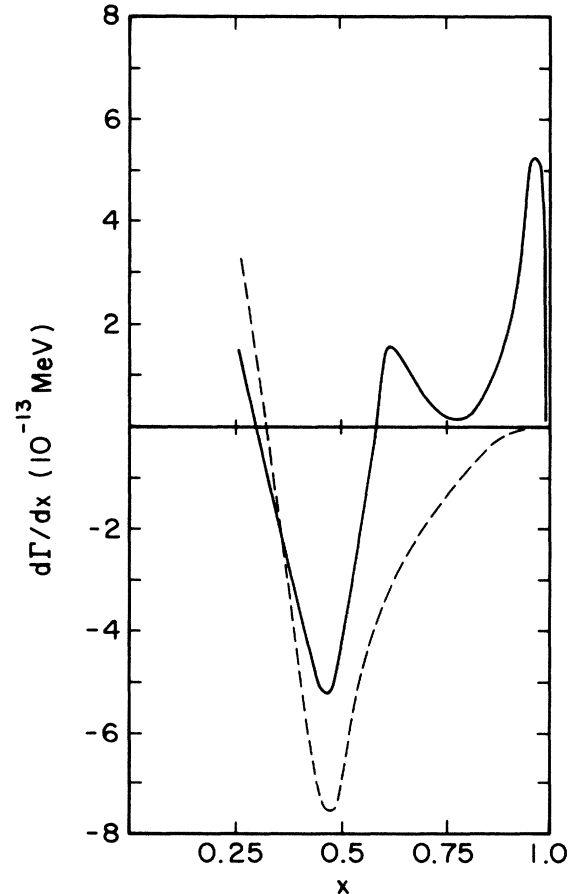


FIG. 6. True distribution in x compared to that of x_{vis} for the order- α radiative corrections. x is shown by the dashed curve; x_{vis} is shown by the solid curve.

NaI detectors is large, $\theta = 156^\circ$, the accumulation near $x_{\text{vis}} = 1$ is kinematically allowed. These effects disappear when the NaI detectors subtend a smaller opening angle θ , since it becomes kinematically impossible to produce events with $x_{\text{vis}} \approx 1$.

When we consider the radiative corrections, we have to add the contributions from the virtual and bremsstrahlung terms, which requires us to choose a value of Δ . Given the fact that we are now cutting out regions of a multibody phase space, we expect the resulting distributions to depend upon the chosen value of Δ . However, we need to choose a small value of Δ to simulate the bremsstrahlung events correctly—so we have used the same value of Δ as above. Since there are other effects, such as detection efficiency, which will smear the distributions in any case, we do not expect a residual sensitivity to Δ to be important. The study of such effects are better left to the experimenters themselves.

In Fig. 6, we compare the radiative corrections to the true x distribution with those of the x_{vis} distribution. The radiative corrections to the former are generally in agreement with the results of the calculations in Ref. 8, i.e., where (cf. Fig. 4) it was shown that for $x > 0.15$ the virtual corrections are larger than the bremsstrahlung corrections, so the total correction is negative. However, the x_{vis} distribution is badly distorted and switches from negative values to positive values at $x_{\text{vis}} \approx 0.6$. The accumulation of events near $x_{\text{vis}} = 1$ has the same explanation as noted above. Note that

the region $x < 0.25$ has been excluded from our plots for two reasons. The first is that the contribution from a slope parameter term, ax , is small there, so this region is uninteresting experimentally. The second reason is that to accurately exhibit the cancellation between the virtual and bremsstrahlung contributions requires us to have small statistical errors on both computations and we did not feel it appropriate to waste computer time on a region which is insensitive to a . Given that terms in a are not included in our analysis, a deviation of experimental points from the combined results of Figs. 5 and 6 should be attributed to the presence of a slope parameter term.

In conclusion, our results clearly indicate that the radiative corrections to the decay $\pi^0 \rightarrow \gamma e^+ e^-$ are quite sensitive to the nature of the experimental detector employed and must be included in the analysis of experimental data to determine the slope parameter a . Our results show that the corrections for large x_{vis} become positive for the TRIUMF detector, which includes the energy of captured photons in the lepton energy measurement. This effect was not present in the experiment performed by Fischer *et al.*, where the radiative corrections for large x were found to be negative.

We would like to thank Dr. J.-M. Poutissou for discussions on the TRIUMF experiment. The Monte Carlo integrations were performed on the ITP Ridge 32. This work was partially supported by the National Science Foundation Grant No. PHY 85-07627.

¹J. Fischer *et al.*, Phys. Lett. **73B**, 359 (1978).

²J. Devons *et al.*, Phys. Rev. **184**, 1356 (1969).

³H. Kobrak, Nuovo Cimento **20**, 1115 (1961).

⁴N. P. Samios, Phys. Rev. **121**, 275 (1961).

⁵J. M. Berman and D. A. Geffen, Nuovo Cimento **18**, 1192 (1960).

⁶G. Barton and B. G. Smith, Nuovo Cimento **36**, 436 (1965).

⁷J.-M. Poutissou (private communication).

⁸K. O. Mikaelian and J. Smith, Phys. Rev. D **5**, 1763 (1972).

⁹K. O. Mikaelian and J. Smith, Phys. Rev. D **5**, 2890 (1972); B. E.

Lautrup and J. Smith, *ibid.* **3**, 1122 (1971); D. Joseph, Nuovo Cimento **16**, 997 (1960).

¹⁰SCHOONSCHIP is an algebraic program written by M. Veltman. See H. Strubbe, Comput. Phys. Commun. **8**, 1 (1974).

¹¹G. B. Tupper, T. R. Grose, and M. A. Samuel, Phys. Rev. D **28**, 2905 (1983).

¹²M. Lambin and J. Pestieau, Phys. Rev. D **31**, 211 (1985).

¹³G. Tupper, Oklahoma State University Report No. 165, 1985 (unpublished); D. Beder (private communication).